Çukurova Üniversitesi
Mühendislik Fakültesi Dergisi
Çukurova University
Journal of the Faculty of Engineering
ISSN: 2757-9255 CİLT/VOLUME: 41 SAYI/ISSUE: 2 HAZİRAN/JUNE 2026

# A New Insight at Wind Speed Prediction; Analysis of Prophet Model and LSTM Models

**Başak ÖZTÜRK** [1,a], **Gülbahar BİLGİÇ TÜZEMEN** [2,b]

[1]*Nevşehir Hacı Bektaş Veli Üniversitesi, Faculty of Engineering-Architecture, Department of Computer Engineering, Nevşehir, Türkiye*
[2]*Nevşehir Hacı Bektaş Veli Üniversitesi, Faculty of Engineering-Architecture, Department of Metallurgical and Materials Engineering, Nevşehir, Türkiye*

[a]***ORCID**: 0000-0002-7295-2452;* [b]***ORCID**: 0000-0002-9503-5884*

**Article Info**
*Received : 10.04.2026*
*Accepted : 14.05.2026*
*DOI: 10.21605/cukurovaumfd.1927153*

**Corresponding Author**
*Başak ÖZTÜRK*
*basakozturk@nevsehir.edu.tr*

**Keywords**
*LSTM*
*Prophet model*
*Renewable energy*
*Wind speed prediction*

***How to cite:*** *ÖZTÜRK, B., BİLGİÇ TÜZEMEN, G., (2026). A New Insight at Wind Speed Prediction; Analysis of Prophet Model and LSTM Models. Cukurova University, Journal of the Faculty of Engineering, 41(2), 479-490.*

**ABSTRACT**

Recently, wind speed (WS) prediction has attracted the interest of clean energy researchers. As WS is inherently uncontrollable, it can cause imbalances between consumption and wind energy production. Therefore, high-accuracy WS estimation is essential. In this study, the LSTM and Prophet models were used to predict future trends based on past WS values obtained from the Nevşehir Meteorology Directorate wind measurement station. Model performances were compared using error metrics. The Prophet model achieved an $R^2$ value of 0.61, while the LSTM model outperformed it with an $R^2$ of 0.734, indicating that the LSTM model's forecasts correspond more closely to actual WS data.

## Rüzgar Hızı Tahminine Yeni Bir Bakış; Prophet Modeli ve LSTM Modellerinin Analizi

**Makale Bilgileri**
*Geliş : 10.04.2026*
*Kabul : 14.05.2026*
*DOI: 10.21605/cukurovaumfd.1927153*

**Sorumlu Yazar**
*Başak ÖZTÜRK*
*basakozturk@nevsehir.edu.tr*

**Anahtar Kelimeler**
*LSTM*
*Prophet modeli*
*Rüzgar hızı tahmini*
*Yenilenebilir enerji*

***Atıf şekli:*** *ÖZTÜRK, B., BİLGİÇ TÜZEMEN, G., (2026). Rüzgar Hızı Tahminine Yeni Bir Bakış; Prophet Modeli ve LSTM Modellerinin Analizi. Çukurova Üniversitesi, Mühendislik Fakültesi Dergisi, 41(2), 479-490.*

**ÖZ**

Son zamanlarda, rüzgar hızı (WS) tahmini temiz enerji araştırmacılarının ilgisini çekmiştir. WS doğası gereği kontrol edilemez olduğundan, tüketim ve rüzgar enerjisi üretimi arasında dengesizliklere neden olabilir. Bu nedenle, yüksek doğrulukta WS tahmini şarttır. Bu çalışmada, Nevşehir Meteoroloji Müdürlüğü rüzgar ölçüm istasyonundan elde edilen geçmiş WS değerlerine dayanarak gelecekteki eğilimleri tahmin etmek için LSTM ve Prophet modelleri kullanılmıştır. Model performansları hata metrikleri kullanılarak karşılaştırılmıştır. Prophet modeli 0,61'lik bir $R^2$ değeri elde ederken, LSTM modeli 0,734'lük bir $R^2$ değeriyle daha iyi performans göstermiş ve LSTM modelinin tahminlerinin gerçek WS verilerine daha yakın olduğunu göstermiştir.

## 1. INTRODUCTION

Accurate estimation of WS is essential for the economical and sustainable functioning of wind turbines [1]. The estimation of WS has garnered significant interest from researchers in the renewable energy industry during the past decade, primarily because of its application in the production of clean energy [2]. Wind energy, a clean, renewable energy source, is rapidly increasing in importance as an alternative and critical source for electricity production. The diversification of renewable energy sources, including solar, wind, and other thermodynamic systems, plays an important role in achieving sustainable energy goals [3]. Increasing wind energy production has a potential and positive impact on energy supply, but has challenges as the output power is uncontrollable, WS and direction dependent, making it difficult to control stable energy production [4]. However, WS characteristics are highly random, fluctuating, and nonlinear, making it difficult for models to make precise predictions [5]. To overcome this, accurate WS and direction predictions are required to subsequently reduce the amount of energy produced. Therefore, finding the correct energy estimation model is becoming increasingly important in solving the above-mentioned issue. So far, many models have been used to predict short- and long-term WS. We can broadly group these as machine learning, artificial intelligence (AI), and hybrid models [1,6]. Machine learning algorithms have been successfully employed in forecasting various renewable energy sources beyond wind, such as hydroelectric power generation [7], confirming the broad applicability of data-driven approaches in renewable energy forecasting. However, these models have several shortcomings, such as slow convergence (traditional), high complexity, etc. As a result of the rapid advancement of advanced measurement technology, a huge amount of data has been collected in recent years. The deep learning neural network called LSTM has managed to solve a wide variety of problems practically by using large amounts of data. Since LSTM can track past events over a long period of time, it offers more comprehensive elements in estimating models. With this feature, LSTM can calculate hidden states using various approaches to produce various predictions. The basic concept of the LSTM model consists of a memory cell and three gates: an entry gate, an exit gate, and a forget gate. The LSTM gate is the only component that interacts with the environment and memory cells. The LSTM model utilizes spatio-temporal properties to capture variations in WS and direction over time in time-series image data. There are several recent studies reviewed in the literature centered on reducing the complexity of wind modeling operations.

Jaseena and Kovoor [8] proposed a bidirectional LSTM-based Ensemble Empirical Mode Decomposition (EEMD)-based WS forecasting system. To forecast WS, the proposed system combines EEMD and Bidirectional LSTM networks. Bidirectional LSTM networks are used to forecast the high-frequency and low-frequency sub-series separately. The forecast results of each sub-series are then combined to obtain the results. High- and low-frequency signals are separated here by two hidden layers of stacked bidirectional LSTM networks.

Sari et al. [9] built a deep learning-based wind predictive technique to facilitate the expansion of wind energy generation. The proposed modelling algorithm aimed to predict wind data as a series of images, expressed as time sequence of images. For this purpose, they used a 3DCNN and a deep convolutional LSTM. In comparison to the 3D-LSTM model, this model is effective in reducing training time and prediction error.

Chen et al. [10] developed a model using EEMD, genetic algorithm (GA), and LSTM algorithms for a short-term WS forecast under large historical wind data. Then, the fine-tuned machine learning model and the heuristically selected feature set were built simultaneously by employing an iterative approach utilizing the combined GA-LSTM technique. As a result, the current model's predictive accuracy was found to be significantly better than that of non-EEMD models, with an average improvement of 56.25%.

Recently, the potential of the Prophet model to predict WS has been discovered. Atasever et al. [11] created the Prophet model, an advanced machine learning model that has not been previously employed in the literature for short-term wind prediction. The results of the developed Prophet model were compared with the results of the Auto-Regressive Integrated Moving Average (ARIMA) model to review the performance reliability and accuracy. In addition, the models' fit and functionality were assessed using partial autocorrelation, autocorrelation function, and standardized residuals. The outcomes demonstrated the prophet model's potential for predicting WS.

Most of the LSTM models mentioned above have disadvantages in building decision models on complex data. For massive and complex datasets running on low-configuration platforms, deep learning models such as CNN-LSTM struggle with both slow computational performance and inappropriate hyperparameter tuning. Traditional models rely heavily on static data for accurate predictions, and modeling becomes very difficult when this data contains a lot of seasonality.

Here, the LSTM model, a deep learning method frequently used in WS prediction, and the Prophet model, a current statistical model, are compared. The proposed study aims to close the technology gap in WS prediction by addressing the shortcomings of existing research. In the study, hourly WS data were trained using LSTM and Prophet models. Performance was then evaluated using sensitivity analysis with mean absolute percent error (MAPE), root mean square error (RMSE) and mean absolute error (MAE).

The average values of the proposed LSTM model forecasts and day-ahead forecasts were found to be 0.701 (RMSE), 0.362 (MAPE), and 0.526 (MAE). According to these prediction values, the LSTM model gave better results than the Prophet model in predicting WS.

## 2. METHOD AND DATA PROCESSING

In this study, historical WS values obtained from wind sensors in the Nevşehir Meteorology Directorate wind measurement station at 1260 m were studied. A one-year data set has been used in many studies on WS prediction in mid-latitudes. Therefore, within the scope of this study, data in a 1-hour interval from January 2020 to March 2021 were studied. WS data collected hourly were split into training (80%) and test (20%) sets prior to model fitting. WS data collected hourly for a year was trained to predict a month of wind data.

Figure 1 shows the presence of spikes in daily WS at every 1-h interval, indicating seasonality. When the WS features in the data set were analyzed, the lowest WS value was found to be 0 m/s, the highest wind value was 19.2 m/s towards the north, and the average WS value was 1.75 m/s. Prior to training, WS values were normalized to the [0, 1] range using min-max scaling and missing values were addressed by linear interpolation. The WS data was modeled using a computer running at 2.80 GHz on an i9 10900 CPU with an operating system and Python 3.9. For the Prophet model, we used an open-source library published by Facebook's Core Data Science team.

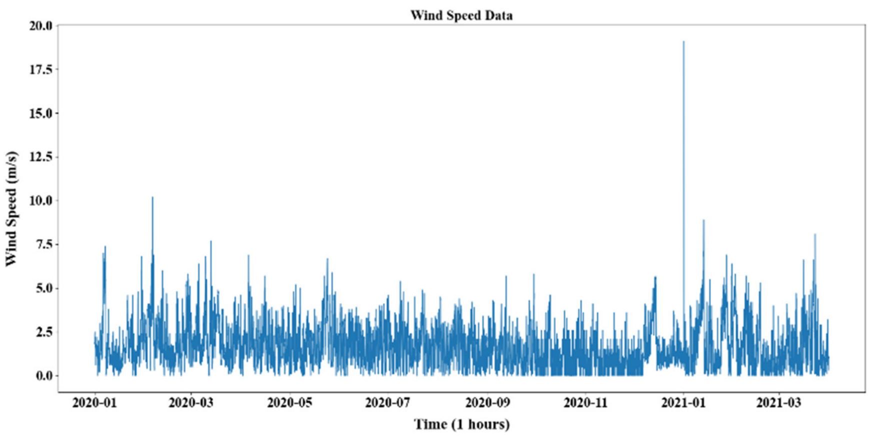


**Figure 1.** Distribution of WS data

A wind rose diagram is a useful tool for understanding wind patterns in a region. This diagram was created by analyzing measured WSs and directions. It provides information by showing the most common wind directions and WSs in different directions. Essentially, the wind rose diagram can give us an overall picture of the wind patterns in a specific location, which can be helpful for a variety of purposes such as planning and designing structures, determining suitable locations for wind energy generation, and more [10].

Additionally, the periodicity of any speed of the WS can be precisely calculated by utilizing the characteristics of the Weibull distribution, which is commonly employed in the study of wind data [12].

The density function known as Weibull is used to display the frequency of wind blowing at various speeds. However, to obtain the Weibull function, some parameters, such as shape and scale, need to be known.

$$f(v) = \frac{k}{c}\left(\frac{v}{c}\right)^{k-1} exp\left[-\left(\frac{v}{c}\right)^{k}\right] \tag{1}$$

In Equation 1, k is the dimensionless form parameter, c is the scale parameter, and f(v) is the Weibull density function at the WS. The following Equation 2, [13], can be used to get the average WS $v_m$ .

$$v_m = \int_0^\infty v f(v) dv = c\Gamma\left(1 + \frac{1}{k}\right) \tag{2}$$

Here, the gamma function can be expressed by the following Equation 3 [14,15].

$$\Gamma(y) = \int_0^\infty e^{-x} x^{y-1} dx \tag{3}$$

## 3. METHODOLOGY

### 3.1. Long Short-Term Memory Network (LSTM)

RNN models are predicted to be a good model for time series processing. However, due to the problem of disappearing the slope, there are problems in learning long-term information. Therefore, Hochreiter and Schmidhuber [16] proposed the LSTM model, which is a special type of RNN. LSTM has been deemed appropriate for time series predicting tasks. Because these networks are succeeded at capturing extended relationships across time by utilizing gates included in each cell of the model (LSTM cell structure representation in Figure 2).

An LSTM network can be briefly described as follows: it has an input layer, an output layer, and a set of recursive hidden layers. Many memory modules form the recursive hidden layer. Three gates that regulate the flow of information (memory gates, forget gates, and output gates) are located in each module, along with one or more independent memory cells [16]. Input Gates (Equation 4) update information and output gates (Equation 6) determine the cell output. The internal state memory cell (Equation 7) offers the internal storage of pertinent prior knowledge and forget gates (Equation 5) decide if the past information is eliminated from a cell state.

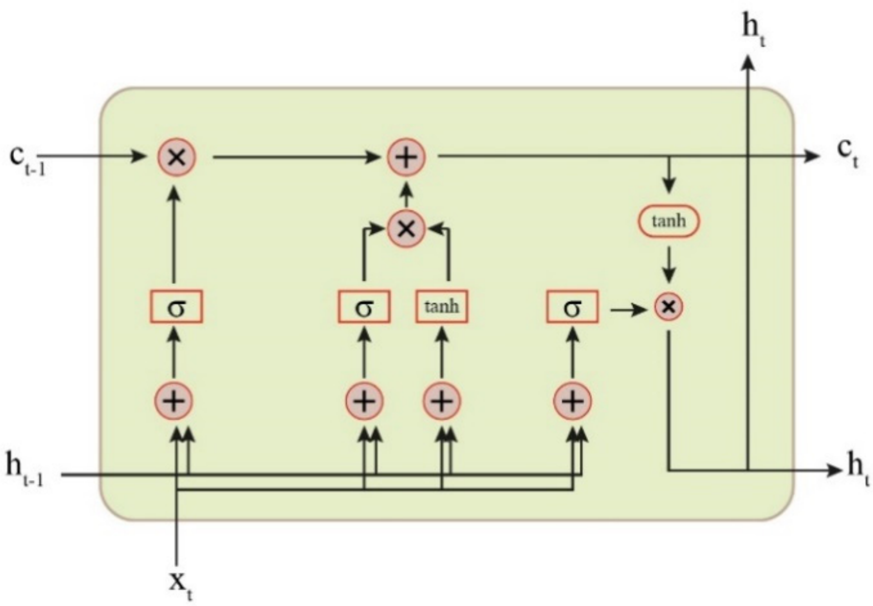


**Figure 1.** Cell structure of LSTM

$$i_t = \sigma(W_i . [h_{t-1} + x_t] + b_i) \tag{4}$$

$$f_t = \sigma\left(W_f . [h_{t-1} + x_t] + b_f\right) \tag{5}$$

$$o_t = \sigma(W_o . [h_{t-1}, x_t] + b_o) \tag{6}$$

$$\widetilde{C}_t = tanh(W_c . [h_{t-1} + x_t] + b_c) \tag{7}$$

$$c_t = \left(i_t * \widetilde{C}_t + f_t * c_{t-1}\right) \tag{8}$$

$$h_t = o_t * tanh(c_t) \tag{9}$$

σ (sigma) is known as the sigmoid activation function and represents the activation of the appropriate gates, $W_f$, $W_i$, $W_o$, $W_c$ are the weight matrices, $b_i$, $b_f$, $b_o$, $b_c$ are the biases values of the corresponding gates, * represents Hadamrd's product, $h_{t-1}$ is hidden state output at time *t-1*, $x_t$ is the input at time *t*, $\widetilde{C}_t$ is the intermediate cell state [17].

### 3.2. The Prophet Models

Facebook's Core Data Science developed the Prophet model to address the typical elements of a commercial time series forecasting model [16]. The Prophet model is quick and entirely automated, but it offers a wide range of customization possibilities for users to improve their forecasts. The Prophet works best with time series that have significant seasonal effects and several seasons of historical data because it is robust against outliers and trend shifts [17]. The original time series' seasonality is preserved by the Prophet model. They constructed a model with changeable heuristic parameters based on a time series model [11] that included three crucial components (trend, seasonality, and vacations). The model consists of four mains. The model consists of four main components: g(t) trend function is given in Equation 11, h(t) holiday, s(t) seasonality is given in Equation 12, and error item Equation 10.

$$y(t) = g(t) + s(t) + h(t) + \varepsilon_t \tag{10}$$

$$g(t) = (k + a(t)^T \delta)t + (m + a(t)^T \gamma) \tag{11}$$

Where k, δ, m and γ represents to the growth rate, adjustment rate, offset parameter, and trend change point in Equation 11. In Equation 12,

$$s(t) = \sum_{n=1}^{N} \left(a_n \cos\left(\frac{2\pi nt}{P}\right) + b_n \sin\left(\frac{2\pi nt}{P}\right)\right) \tag{12}$$

Here, the seasonality period is defined by P. Daily, weekly, and annual seasonality are the periodic changes that reflect the seasonality function, s(t). The dataset for the Prophet model needs to be a two-column data frame 'ds' (timestamp) and 'y' (prediction measure). The 'ds' column should contain the dates or timestamps for each data point and the 'y' column should contain the corresponding measurement values. The data frame generated after the prediction of the Prophet model contains 'ds' and 'yhat' columns. The 'yhat' column contains the estimated 'y' values for each timestamp in the 'ds' column. In time series forecasting studies, analyzing the data well and determining the model parameters correctly are the most important factors affecting the results. Within the scope of this study, various statistical information and analyses of wind data are detailed in Figure 1 and Table 3. In the selection of the model parameters, the possible parameters were evaluated with the grid system by comparing the RMSE value. The models were finally run with the parameters that gave the lowest error value. The running time of the final model for the LSTM was 23.01727 minutes, while for the Prophet model it was 11.0723 minutes. Parameters determined to be appropriate for the models are listed in Table 1.

Since time series prediction is to be done in this study, LSTM and Prophet were preferred as learning techniques for the data. The window size was tried with 4, 12, and 24 and set to the appropriate value of 12. A 3-layer LSTM architecture was built. The number of neurons for each LSTM layer in this architecture is given in Table 1.

LSTM optimization is the process of finding the optimal parameter values for a given problem. Various optimization algorithms such as RMSprop, Adadelta and Adam have been widely used in such systems. The dropout technique has been used to avoid overfitting in the learning process and to improve prediction accuracy. Dropout aims to prevent overlearning by randomly stopping some neurons from firing. In this study, a dropout rate of 0.2 is used. The most useful parameter for predicting the trend's flexibility and how much it will fluctuate at trend change points is "changepoint prior scale." The modeling of trend changes is insufficient if this parameter is maintained too little, while the trend is excessive if it is kept too big. The default value of this parameter is 0.05 but this could be tuned in the range of [0.001, 0.5].

**Table 1.** Model parameters of LSTM and Prophet model

| Models | Parameters | Quantity |
|---|---|---|
| **LSTM** | number of hidden layers | 3 |
| | number of time steps | 12 |
| | batch size | 64 |
| | number of neurons in layers | 100,100,50 |
| | epoch size | 200 |
| | optimizer | RMSprop |
| | learning rate | 0.01 |
| **The Prophet model** | changepoint prior scale | 0.001 |
| | changepoint range | 0.9 |
| | seasonality prior scale | 0.01 |
| | seasonality mode | multiplicative |
| | growth | logistic |

"changepoint range" determines the historical ratio to be taken into account when determining the trend value. We used this parameter, which has values between [0.8 and 0.95], as 0.9 in this study. This value represents the past 90% of the time series. The elasticity of seasonality is controlled by the 'seasonality prior scale' parameter. If the value is small, seasonality is reduced; if it is large, it can adapt to large fluctuations. In our time series, seasonality mode exhibits multiplicative seasonality. This indicates if the magnitude of the seasonal variations is influenced by the length of the time series. Given that the time series shows forward growth, the growth parameter was employed as a logistic.

### 3.3. Numerical Simulation and Validation

This paper presents an approach that integrates Prophet and LSTM models to estimate WS. Some classical evaluation criteria, such as mean square error (MSE), RMSE, MAPE, MAE, and $R^2$ were used to evaluate the performance results of LSTM and Prophet models. These metrics are expressed mathematically using Equations [16-20].

$$MSE = \frac{1}{N}\sum_{i=1}^{N}(y_i - \tilde{y}_i)^2 \tag{13}$$

$$RMSE = \sqrt{MSE} \tag{14}$$

$$MAE = \frac{1}{N}\sum_{i=1}^{N}|\tilde{y}_i - y_i| \tag{15}$$

$$MAPE = \frac{1}{N}\sum_{i=1}^{N}\frac{|\tilde{y}_i - y_i|}{y_i} \tag{16}$$

$$R^2 = 1 - \frac{\sum_{i=1}^{N}(y_i - \tilde{y}_i)^2}{\sum_{i=1}^{N}\left(y_i - \underline{y}\right)^2} \tag{17}$$

Where N is the number of WS data evaluated, $y_i$, $\tilde{y}_i$ and $\underline{y}$ represents the original, the predicted, and the mean values of the WS.

## 4. RESULTS AND DISCUSSION

The stages of the seasonal LSTM and Prophet models are presented in Figure 3. The required model parameters are first computed following the creation of a tentative model. This parameter estimation's primary objectives are to lower the prediction error and ascertain the model's order and parameters. RMSE is determined by taking the square root of MSE; MSE is the squared difference between actual and observed values. MAE is defined as the absolute difference between actual and observed values. MAPE provides data analysis by calculating the percentage difference between actual values and predicted values. Table 2 shows $R^2$, which describes the fitness match of the prediction results of the LSTM and Prophet model to the actual values. The higher the $R^2$ value, the higher the prediction accuracy. Therefore, lower values of MAE, MAPE, and RMSE are a measure of better forecasting performance.

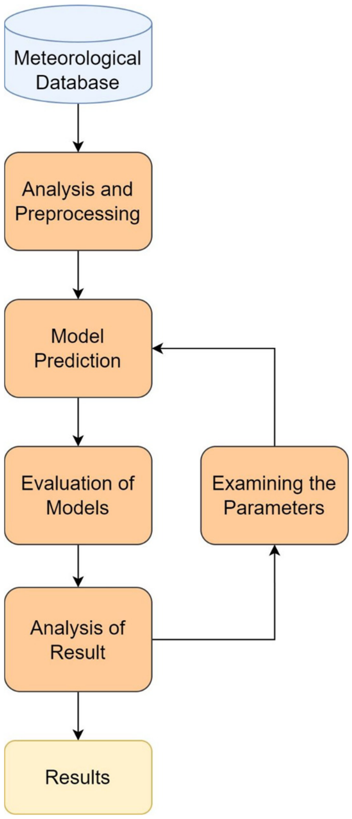


**Figure 3.** Flowchart for the Prophet and LSTM model construction process

**Table 2.** Model evaluation metrics

| Predicted models | Evaluating metrics | | | | |
|---|---|---|---|---|---|
| | MSE | RMSE | MAE | MAPE | $R^2$ |
| **LSTM** | 0.492 | 0.701 | 0.526 | 0.362 | 0.734 |
| **The Prophet model** | 1.35 | 3.17 | 1.78 | 1.39 | 0.61 |

An example of actual and predicted WS using LSTM and Prophet is shown in Figures 4 and 5. Figure 4 demonstrates how well the LSTM's predicted WS matches the actual WS. Figure 4 shows that the speed predicted by LSTM is significantly different from the observed value over a wide time range. $R^2$ value found in this context is 0.73. The variance and mean of wind data have remained consistent despite sudden ups and downs over time. This situation prevented the Prophet model from obtaining a lower error value.

As a result, it demonstrates that, compared to other models, the LSTM's anticipated WS is virtually more proximate to the actual WS. It demonstrates how the LSTM performs better than other models.

The relationship between the real and predicted WS's demonstrates how much closer the forecast is to the actual WS. The correlation score is between 0 and 1. When the correlation is 1, the WS predicted, and reality are both the same. When the correlation is zero, it means that the actual and predicted WS's are not the same. Figure 5 shows how well Prophet's predicted WS matches the actual WS. The $R^2$ coefficient of determination was found to be 0.61. This proves the matching of this model. The model indeed accurately predicts the unpredictability of the data, yet some discrepancies are noticed in the sharp peaks and valleys. Based on the RMSE and MAE results, the LSTM model performs better than the Prophet model (see Figures 4 and 5).

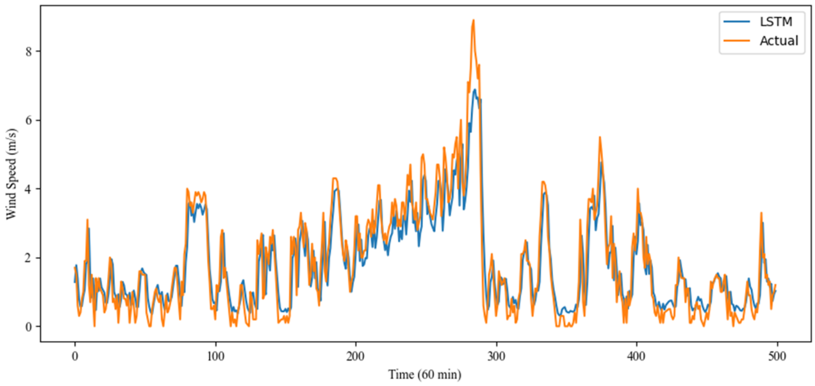


**Figure 4.** WS predictions for the LSTM

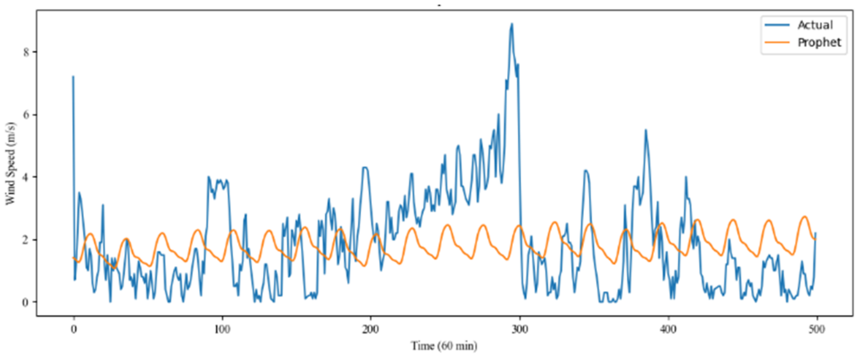


**Figure 5.** WS predictions for the Prophet model

Prior studies have commonly indicated that the Prophet model exhibits superior forecasting capabilities compared to the SARIMA (5,0,0) (0,1,0) model [11]. However, in this study, due to higher error rates, the Prophet model yielded less precise forecasts when compared to the LSTM model.

Figure 6 shows the comparison of Prophet model and LSTM model prediction results and WS actual data. As can be seen in the figure, it shows that the predicted WS of LSTM is almost closer to the actual WS compared to the Prophet model. This shows how LSTM outperforms the other model.

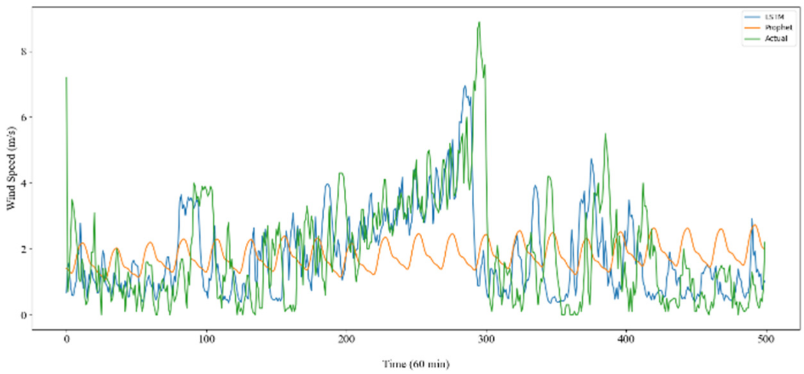


**Figure 6.** Comparison of Prophet and LSTM model WS prediction results and actual data

Figure 7 illustrates how wind roses, which are typically used to describe wind distributions of various speeds and directions, work. These graphs demonstrate how, at three locations, the eight primary wind directions vary from a month typical of one season to a month typical of another season, [13,21]. The wind rose diagram created using hourly collected WS and wind direction in 2021 is shown in the figure. The diagram shows that the prevailing wind direction of the region is mainly N and S. The results of the WS and direction measurements at 60 m are depicted in Figure 7.

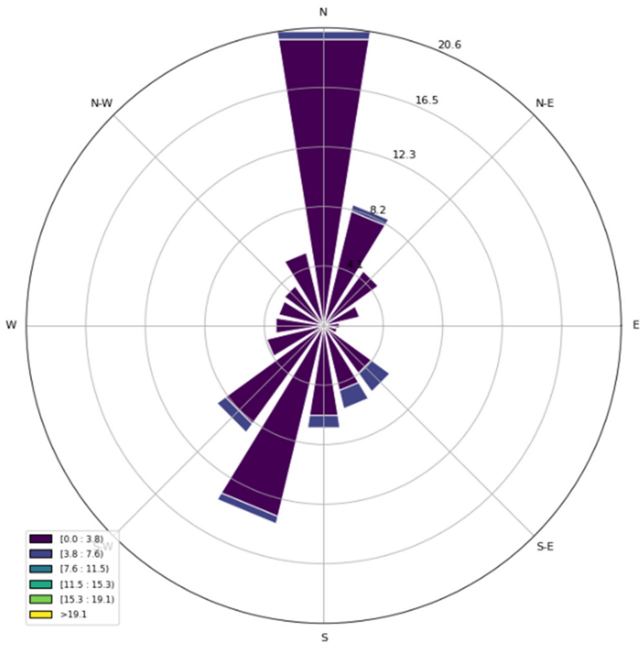


**Figure 7.** An annual wind rise graphic at a height of 60 meters

Details on the distributions of WS and direction at a particular station are offered in Table 3. The analytical approach involved both counting the calms and computing the mean and variation of the non-calm observations made at the station each month, utilizing all of the 24-hour data collected over the course of a year. Then, using the linear regression technique, the monthly Weibull distribution parameters c and r were determined. Table 3 displays the results. It is important to note that calms occur often at Nevşehir all year long as well as at Ioannina from April to November and from February to October. If not, they are uncommon. Weibull distribution pattern and scale parameters of the region were obtained as 0.155 and 1.742 m/s.

**Table 3.** Average monthly mean WS with Weibull parameters (for 60 m)

| Mounth | Weibull distribution | | | Actual V(m/s) |
|---|---|---|---|---|
| | V(m/s) | c | k | |
| **January** | 0.135 | 0.452 | 1.397 | 1.840 |
| **February** | 0.090 | 0.804 | 1.480 | 2.285 |
| **March** | 0.130 | 0.933 | 1.288 | 2.221 |
| **April** | 0.144 | 0.799 | 1.143 | 1.943 |
| **May** | 0.149 | 0.717 | 1.315 | 2.033 |
| **June** | 0.001 | 0.811 | 0.967 | 1.778 |
| **July** | 0.184 | 0.786 | 1.038 | 1.825 |
| **August** | 0.221 | 0.666 | 1.033 | 1.699 |
| **September** | 0.171 | 0.468 | 1.038 | 1.507 |
| **October** | 0.001 | 0.236 | 0.957 | 1.194 |
| **November** | 0.001 | 0.201 | 0.785 | 0.987 |
| **December** | 0.174 | 0.462 | 1.133 | 1.596 |
| **Average** | 0.155 | 0.611 | 1.131 | 1.742 |

## 5. CONCLUSION

This article presents a comparative example of the Prophet model and the LSTM model. These models were applied by modeling real-time WS data with the parameters in Table I. Simulation results corroborate that the LSTM model has the lowest values of RMSE, MAE, and MAPE in comparison to the Prophet model. The results obtained for the day-ahead predictions of the proposed LSTM model are 0.701 (RMSE), 0.362 (MAPE), and 0.526 (MAE), respectively, while the Prophet model yields values of 3.17 (RMSE), 1.39 (MAPE), and 1.78 (MAE). This prediction values obtained for LSTM are lower than those of the Prophet model. Consequently, this study demonstrates that using the LSTM model to accurately predict WS yields better results than the Prophet model.

A summary of works that compare suggested models or employ LSTM and Prophet in the literature is given in Table 4. As a result, with the increase in neural network model studies, many advanced approaches have been developed to process nonlinear data. An important component affecting Prophet's performance is the distribution of wind speed values evaluated with the Weibull distribution. The analysis, which incorporates a Weibull probability density function (PDF) plot in Figure 7 and Table 3, reveals that the dataset shows a heavy-tailed distribution, indicating the presence of outliers. Given that Prophet presumes additive seasonal patterns and trends, it may have difficulties in accurately representing the nonlinear dynamics and sudden fluctuations inherent in data. Furthermore, the WS variations in the dataset display significant short-term oscillations and non-stationary characteristics, complicating Prophet's time series decomposition's ability to generalize well. In contrast to financial or economic time series, WS data is intrinsically stochastic, resulting in heightened uncertainty in model projections. Therefore, although the proposed LSTM and Prophet methods perform adequately, a suitable prediction strategy is still needed to handle and resolve unexpected changes in the dataset. Therefore, it would be more appropriate to apply hybrid methods. In our future work, hybrid methods using different deep learning models and different algorithms will be tried for WS prediction. Furthermore, research that employs different parameter selection and metaheuristic optimization techniques to make this more efficient and relevant will be covered.

**Table 4.** An overview of the research that compares or uses LSTM and Prophet

| Method | RMSE | MAE | Data type | Ref. |
|---|---|---|---|---|
| **Conv-LSTM** | Set 1: 0.380<br>Set 2: 0.275<br>Set 3: 0.249 | Set 1: 0.279<br>Set 2: 0.154<br>Set 3: 0.176 | WS Data | [22] |
| **EMD-GA-LSTM** | 0.1337 | 0.0570 | WS Data | [8] |
| **LSTM** | Set 1: 2.18<br>Set 2: 2.13<br>Set 3: 0.85<br>Set 4: 1.03 | Set 1: 1.65<br>Set 2: 1.74<br>Set 3: 0.59<br>Set 4: 0.69 | WS Data | [23] |
| **LSTM** | 0.088 | 0.084 | WS Data | [24] |
| **LSTM** | Dataset 1: 0.558<br>Dataset 2:0.532<br>Dataset 3:0.194 | - | WS Data | [25] |
| **LSTM** | 3.124 | 2.457 | WS Data | [2] |
| **Feature-LSTM** | 0.1745 | 0.1212 | WS Data | [1] |
| **PSO-VMD-Bi-LSTM** | - | 0.194 | WS Data | [5] |
| **LSTM** | 0.701 | 0.526 | WS Data | This study |
| **Prophet** | 957.583 (for Turkey)<br>5,574.244 (for Japan) | 706.916 - (Regarding Turkey)<br>4,921.811 (Regarding Japan) | Energy consumption | [26] |
| **Prophet** | 3.78-45.80 (General Prophet model) 3.54-39.86 (Log Prophet model) | - | Odisha health care data (Air Pollution) | [27] |
| **Prophet** | 3.17 | 1.78 | WS Data | This study |

## 6. REFERENCES


1. Geng, D., Zhang, H. & Wu, H. (2020). Short-term wind speed prediction based on principal component analysis and LSTM. *Applied Sciences, 10*(13), 4416.
2. Elsaraiti, M. & Merabet, A. (2021). A comparative analysis of the ARIMA and LSTM predictive models and their effectiveness for predicting wind speed. *Energies, 14*(20), 6782.
3. Kaplan, A. & Özbek, A. (2022). Exergy analysis of a double-stage organic Rankine cycle using renewable energy. *Çukurova Üniversitesi Mühendislik Fakültesi Dergisi, 37*(1), 43-54.
4. Biçen, T., Arslan, A.A. & Vardar, A. (2022). Regional solar and wind energy characteristics and its energy potential in northwest of Turkey. *Gümüşhane University Journal of Science and Technology, 12*(2), 527-538.
5. Li, J., Song, Z., Wang, X., Wang, Y. & Jia, Y. (2022). A novel offshore wind farm typhoon wind speed prediction model based on PSO–Bi-LSTM improved by VMD. *Energy, 251*, 123848.
6. Santur, Y. (2020). Deep learning based regression approach for algorithmic stock trading: A case study of the BIST30. *Gümüşhane Üniversitesi Fen Bilimleri Dergisi, 10*(4), 1195-1211.
7. Atalay, B.A. ve Zor, K. (2025). XGBoost (aşırı gradyan artırımlı karar ağaçları) ile hidroelektrik enerji tahmini. *Çukurova Üniversitesi Mühendislik Fakültesi Dergisi, 40*(1), 205-218.
8. Jaseena, K.U. & Kovoor, B.C. (2021). EEMD-based wind speed forecasting system using bidirectional LSTM networks. *2021 International Conference on Computer Communication and Informatics (ICCCI), Coimbatore*, India, 1-9.
9. Sari, A.P., Suzuki, H., Kitajima, T., Yasuno, T., Prasetya, D.A. & Arifuddin, R. (2022). Short-term wind speed and direction forecasting by 3DCNN and deep convolutional LSTM. *IEEJ Transactions on Electrical and Electronic Engineering, 17*(11), 1620-1628.
10. Chen, Y., Dong, Z., Wang, Y., Su, J., Han, Z., Zhou, D., Zhang, K., Zhao, Y. & Bao, Y. (2021). Short-term wind speed predicting framework based on EEMD-GA-LSTM method under large scaled wind history. *Energy Conversion and Management, 227*, 113559.
11. Atasever, S., Öztürk, B. & Bilgiç, G. (2022). A new approach to short-term wind speed prediction: the Prophet model. *Energy Sources, Part A: Recovery, Utilization, and Environmental Effects, 44*(4), 8826-8841.
12. Rehman, S. & Al-Abbadi, N.M. (2008). Wind shear coefficient, turbulence intensity and wind power potential assessment for Dhulom, Saudi Arabia. *Renewable Energy, 33*(11), 2653-2660.
13. Fyrippis, I., Axaopoulos, P.J. & Panayiotou, G. (2010). Wind energy potential assessment in Naxos Island, Greece. *Applied Energy, 87*(2), 577-586.
14. Katsoulis, B.D. & Metaxas, D.A. (1992). The wind energy potential of western Greece. *Solar Energy, 49*(6), 463-476.
15. Oral, F. & Behçet, R. (2015). Rüzgar verilerinin enerji üretimi amaçlı değerlendirilmesi. *Bitlis Eren Üniversitesi Fen Bilimleri Dergisi, 4*(2), 173-182.
16. Hochreiter, S. & Schmidhuber, J. (1997). Long short-term memory. *Neural Computation, 9*(8), 1735-1780.
17. Toharudin, T., Pontoh, R.S., Caraka, R.E., Zahroh, S., Lee, Y. & Chen, R.C. (2021). Employing long short-term memory and Facebook Prophet model in air temperature forecasting. *Communications in Statistics - Simulation and Computation, 52*(2), 279-290.
18. Facebook (n.d.). *Prophet | Forecasting at scale.* https://facebook.github.io/prophet/, Access date: June 2026.
19. Aditya Satrio, C.B., Darmawan, W., Nadia, B.U. & Hanafiah, N. (2021). Time series analysis and forecasting of coronavirus disease in Indonesia using ARIMA model and PROPHET. *Procedia Computer Science, 179*, 524-532.
20. Harvey, A.C. & Peters, S. (1990). Estimation procedures for structural time series models. *Journal of Forecasting, 9*(2), 89-108.
21. Ahmed, A.S. (2021). Technical and economic feasibility of the first wind farm on the coast of Mediterranean Sea. *Ain Shams Engineering Journal, 12*(3), 2145-2151.
22. Chen, G., Li, L., Zhang, Z. & Li, S. (2020). Short-term wind speed forecasting with principle-subordinate predictor based on Conv-LSTM and improved BPNN. *IEEE Access, 8*, 67955-67973.
23. Liu, H., Mi, X. & Li, Y. (2018). Smart multi-step deep learning model for wind speed forecasting based on variational mode decomposition, singular spectrum analysis, LSTM network and ELM. *Energy Conversion and Management, 159*, 54-64.

**24.** Rodrigues Moreno, S., Gomes da Silva, R., Cocco Mariani, V. & dos Santos Coelho, L. (2020). Multi-step wind speed forecasting based on hybrid multi-stage decomposition model and long short-term memory neural network. *Energy Conversion and Management, 213*, 112869.

**25.** Zhang, Z., Ye, L., Qin, H., Liu, Y., Wang, C., Yu, X., Yin, X. & Li, J. (2019). Wind speed prediction method using shared weight long short-term memory network and Gaussian process regression. *Applied Energy, 247*, 270-284.

**26.** Samal, K.K.R., Babu, K.S., Das, S.K. & Acharaya, A. (2019). Time series based air pollution forecasting using SARIMA and Prophet model. *Proceedings of the 2019 International Conference on Information Technology and Computer Communications (ITCC 2019)*, 80-85.

**27.** Arslan, S. (2022). A hybrid forecasting model using LSTM and Prophet for energy consumption with decomposition of time series data. *PeerJ Computer Science, 8*, e1001.